Fluctuation theorem for a single particle in a moving billiard: Experiments and simulations

Malte Schmick,[1] Qi Liu,[2] Qi Ouyang,[2] and Mario Markus[1,*]
[1]*Max-Planck-Institut für molekulare Physiologie, Postfach 500247, 44202 Dortmund, Germany*
[2]*Department of Physics, Peking University, Beijing 100871, People's Republic of China*
(Received 12 April 2007; revised manuscript received 22 June 2007; published 21 August 2007)

A single particle within a periodically driven Sinai-billiard-like system is tracked experimentally and is simulated via hard-sphere molecular dynamics. Both experiments and simulations confirm the fluctuation theorem (FT); thus, in this setup, one driven particle is sufficient for the FT to hold. Furthermore, in the simulations the chaoticity of the system can be adjusted using the restitution coefficient of collisions. It is also shown that the FT breaks down when unstable periodic orbits appear for small restitution coefficients.

DOI: 10.1103/PhysRevE.76.021115 PACS number(s): 05.70.Ln, 05.45.−a, 02.60.Jh

I. INTRODUCTION

The fluctuation theorem (FT) can be considered a generalization of the second law of thermodynamics for finite systems (for reviews, see [1,2]) and is of fundamental importance in biochemical motors and nanomachines [3]. It was first shown to hold for shear-flow simulations [4] and for time-reversible chaotic Anosov systems consisting of many particles [5]. Later on, the FT was verified numerically in a number of systems, such as an electrical conduction device [6], coupled oscillators [7,8], and the shell model of turbulence [9]. Also, calculations were reported [10–14] in which it was shown that the source of disorder may not necessarily be a large number of particles, but stochasticity (see discussions in [11,15,16]).

Experimental verifications of the FT have been reported for (i) fluctuations in turbulent flows of fluids [17–19]; (ii) a Brownian particle in an optical trap [15,20]; and (iii) voltage fluctuations of a resistor [21]. It is noteworthy that there have been experiments which showed that the FT is valid for spatial scales of everyday life, namely, in a granular medium consisting of an ensemble of shaken glass beads [22].

Further loosening of the conditions for the FT was found in simulations of a system that neither consists of many particles nor requires stochasticity. This sytem consists of a single particle that is shaken chaotically in a Duffing potential [23]. However, we found this setup difficult to implement experimentally. We therefore devised another one-particle, nonstochastic system, which we will describe in the present work. For this device, we will check the following formulation of the FT, which was also used in [23]:

$$\frac{p(J_\tau)}{p(-J_\tau)} = e^{J_\tau \tau/\beta_\tau}. \tag{1}$$

$p(J_\tau)$ is the probability of the mean flux J_τ (of work, momentum, heat, etc.) during the time τ. Here, we consider the mean flux of the work W_τ, i.e., the mean power $J_\tau = W_\tau/\tau$, where W_τ is the work performed within the time τ by the system in a steady state, where transients from initial conditions have decayed.

*markus@mpi-dortmund.mpg.de

II. EXPERIMENTS

The experimental setup is shown in Fig. 1. In the lower part of the figure one sees a so-called gyratory mixer (GM 1, Ratek Instruments, Australia), which moves the box (darker part of Fig. 1) that is placed above it. The box's movement caused by the gyratory device is a precession around verticality (frequency f, angle α) of an imaginary perpendicular line fixed at the center of the box's bottom. In the present work, we set $f=0.6$ Hz and $\alpha=5°$. The box contains 4×4 cylindrical steel pins (diameter 0.5 cm; height 1.5 cm), which are fixed equidistantly on the bottom (distance between pins, $d=3.75$ cm; distance between pins and the box's wall, $d/2$). A steel wall (height 1.5 cm) surrounds the box.

A glass sphere (white in Fig. 1; diameter 1.2 cm; mass $m=2.21$ g) is placed in the box. A chaotic motion of the sphere is expected due to the divergence of nearby trajectories owing to collisions between convex surfaces. The sphere was monitored by video equipment with 278 frames per second. The experiments lasted $T=12$ h, i.e., 1.2×10^7 frames were recorded. We determined

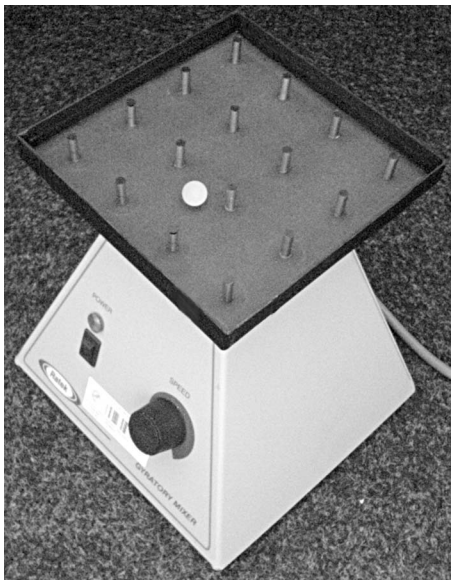

FIG. 1. Experimental setup. A motor in the lower part causes a precession of the darker, upper box with 4×4 fixed cylindrical pins and a moving sphere.

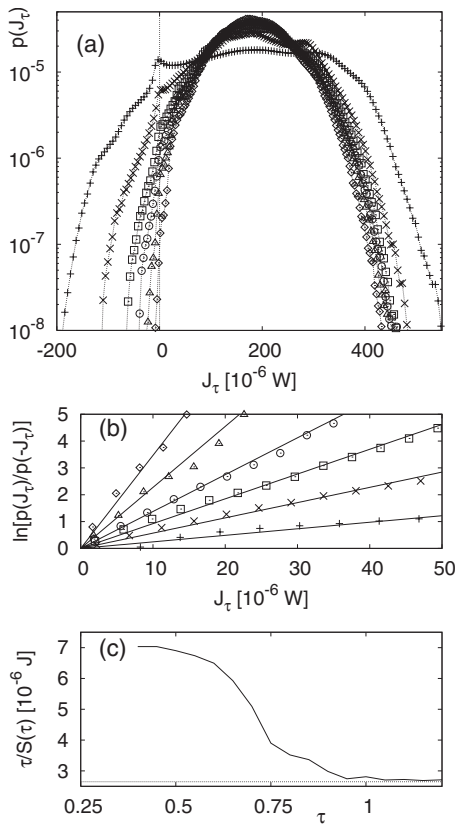

FIG. 2. Experimental results. τ=0.1 (+), 0.4 (×), 0.6 (□), 0.7 (○), 0.8 (△), and 1.0 s (◇). (a) Probability distributions of the mean power J_τ. (b) Plot of $\ln[p(J_\tau)/p(-J_\tau)]$ vs J_τ, as obtained from (a). (c) $\beta_\tau=\tau/S_\tau$ vs τ, where S_τ are the slopes of the straight lines shown in (b).

$$J_\tau = \frac{1}{\tau}\int_t^{t+\tau} \vec{F}\cdot\vec{v}\,dt \tag{2}$$

for a given time τ. $\vec{v}$ is the velocity, which was calculated from the positions of the sphere in successive frames. $\vec{F}$ is the gravitational force

$$\vec{F} = mg\,\sin(\alpha)\begin{pmatrix}\sin(\phi)\\ \cos(\phi)\end{pmatrix}\begin{pmatrix}\hat{x}\\ \hat{y}\end{pmatrix}, \tag{3}$$

where $\hat{x}$ and $\hat{y}$ are the unit vectors on the bottom of the box and $\phi=2\pi ft+\phi_0$ is the angle of the line connecting the lowest point of the box with its center. For highest precision, ϕ was determined, as a function of time, by video monitoring the rotating motion of the corners of the box.

Figure 2(a) shows the probability distribution function $p(J_\tau)$, as determined from the measurements. The parts of the curves with negative J_τ become smaller as τ increases, as expected from the "classical" second law of thermodynamics. For a quantitative check of the FT, as given by Eq. (1), $\ln[p(J_\tau)/p(-J_\tau)]$ was plotted versus J_τ in Fig. 2(b). We obtained linear relationships, confirming Eq. (1). According to this equation, the slopes S_τ of the fitted straight lines [exemplified in Fig. 2(b)] should be given by $S_\tau=\tau/\beta_\tau$. Therefore, $\beta_\tau=\tau/S_\tau$ was plotted versus τ in Fig. 2(c). One sees a monotonically decreasing dependence $\beta_\tau(\tau)$, saturating at large τ to a value $\beta_\infty \approx 2.7\times 10^{-6}$ J.

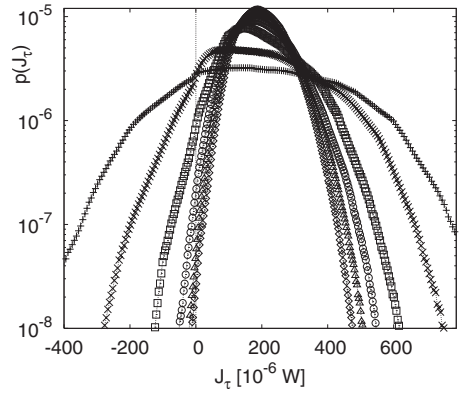

FIG. 3. Simulated probability distribution of the mean power J_τ. τ=0.05 (+), 0.2 (×), 0.4 (□), 0.6 (○), 0.8 (△), and 1.0 s (◇). $e_p=e_w=0.5$.

III. SIMULATIONS

We approximated the system by performing calculations in two dimensions, the sphere being considered as a circle with the same diameter. Also, the dimensions of the box and the pins, as well as the duration T of the evaluated process, were the same as in the experiments. The circle was assumed to move without friction and without rotation. Hard-sphere simulations were used, i.e., a collision changes the momentum instantaneously. After a collision of the circle with a pin or with the wall, the component of the velocity of the sphere perpendicular to the pin's surface or the wall was multiplied by the corresponding restitution coefficient [e_w (e_p) for collisions with the wall (pins)]. As time step of integration we chose $dt=10^3 s$, and found no significant change in the resulting distributions when changing dt.

Figure 3 shows an example of a simulated set of typical distributions $p(J_\tau)$. Figure 4 shows four examples of linear relationships of $\ln[p(J_\tau/p)(-J_\tau)]$ versus J_τ, confirming the

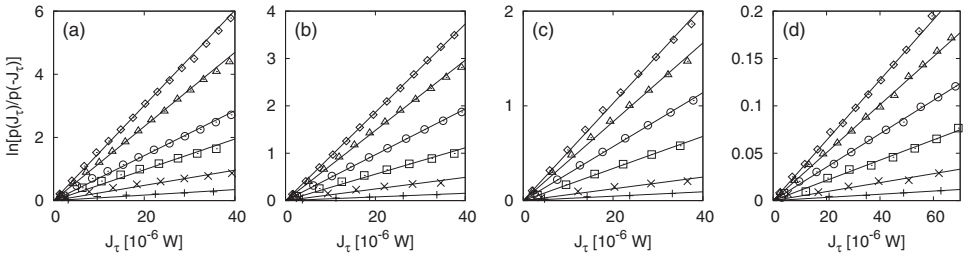

FIG. 4. Linear fits to $\ln[p(J_\tau)/p(-J_\tau)]$ vs J_τ (simulations). Symbols for different τ are as in Fig. 3. (a) $e_p=e_w=0.5$; (b) $e_p=e_w=0.7$; (c) $e_p=0.7$, $e_w=1$; (d) $e_p=1$, $e_w=0.975$.

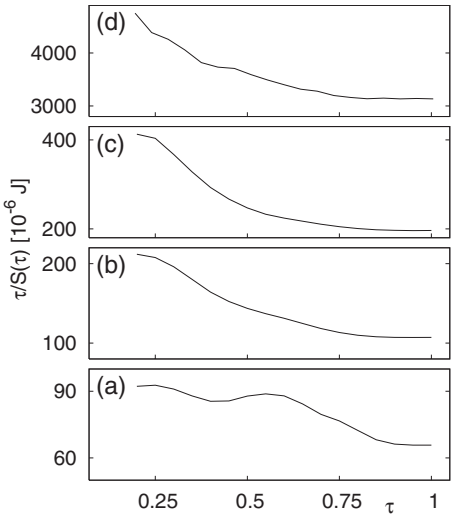

FIG. 5. Plots of $\beta_\tau = \tau/S_\tau$ vs τ, where S_τ are the slopes of the straight lines shown in Fig. 4 (simulations). e_p, e_w for (a)–(d) are as in Figs. 4(a)–4(d), respectively.

FT, as given by Eq. (1). Figure 4(a) corresponds to Fig. 3. Elasticity is increased in Fig. 4(b). In Fig. 4(c) we assume a perfectly elastic wall, i.e., $e_w=1$. This last situation could be compared to that of a Sinai billiard, where collisions with the wall are equivalent to an absent wall and an infinite number of pins behind it; however, due to the inclination of the box, the Sinai-billiard analogy is only an approximate characterization. Figure 4(d) shows the results for (almost) complete elasticity for all collisions ($e_p=1$ and $e_w=0.975$). Note that complete elasticity, i.e. $e_w=e_p=1$, gives $p(J_\tau)$ curves that are symmetrical with respect to $J_\tau=0$, i.e., the left side of Eq. (1) collapses to 1. Figure 5 shows that β_τ saturates for large τ to a value β_∞ in the four evaluated cases, as was also shown experimentally in Fig. 2(c).

β_∞ has been considered as the "effective temperature" of a system [9,22]. In view of this, we determined β_∞ versus the mean kinetic energy $\langle E_{kin}\rangle$ of the sphere, as shown in Fig. 6. In order to alter $\langle E_{kin}\rangle$, we varied e_p and e_w, considering that increasing e_p or e_w decreases dissipation and thus increases $\langle E_{kin}\rangle$. As shown in Fig. 6, we chose three different paths toward elasticity in the e_w-e_p plane, all three yielding very similar results. In other words, the dependence β_∞ vs $\langle E_{kin}\rangle$ is robust with respect to the internal mechanism that changes $\langle E_{kin}\rangle$.

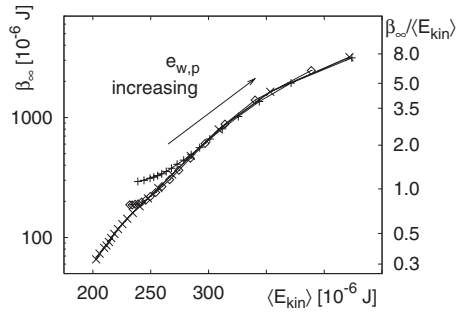

FIG. 6. β_∞ (left ordinate) versus the mean kinetic energy $\langle E_{kin}\rangle$. e_p and e_w are increased from left to right in the following ways: $e_p=e_w$ from 0.5 to 0.975 (×); $e_w=1$, e_p from 0.5 to 0.95 (◇); $e_p=1$, e_w from 0.5 to 0.95 (+). Right ordinate: $\beta_\infty/\langle E_{kin}\rangle$ for $e_p=e_w$ (×).

An analysis of the residence distribution of the particle on the plane showed that such a distribution is correlated with the validity of the FT. This finding is illustrated in Fig. 7. Figure 7(a) shows the spatial distribution for the experiment corresponding to Fig. 2. This distribution reveals deviations from homogeneity, especially near the wall. In contrast, simulations with $e_p>0.6$ and $e_w>0.6$, e.g., in the cases of Figs. 4(b)–4(d), give a homogeneous spatial distribution like the one shown in Fig. 7(b). Simulations with lower restitution coefficients, e.g., $e_p=e_w=0.5$ [case of Fig. 4(a)], do yield spatial inhomogeneities comparable to those in experiments [Fig. 7(c)]. Note, however, that such inhomogeneities do not cause breakdown of the FT, as demonstrated by the linearity of the plots in Fig. 4(a) (simulations) and Fig. 2(b) (experiments). Finally, Figs. 7(d) and 7(e) show simulated distributions, where clearly unstable trajectories are present, which are frequently visited and thus appear as dark curves. As shown by the breakdown of the corresponding linear plots (see Fig. 8), these cases are not associated with validity of the FT. We found such a failure of the FT to occur for sufficiently low values of e_p or e_w.

After scanning the parameter plane defined by e_w and e_p in the simulations, we can sum up the results (exemplified above) as follows. High elasticity yields homogeneous spatial distributions and validity of the FT. Lowering of the elasticity causes inhomogeneous distributions without loss of the validity of the FT; this is also the case in experiments. Extreme lowering of the elasticity causes the appearance of unstable trajectories and failure of the FT. Apparently, the

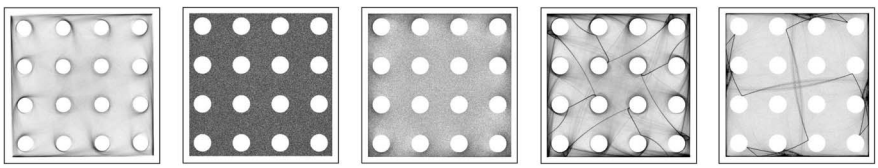

FIG. 7. Spatial distribution of the position of the sphere's center, obtained by averaging over 12 h. The surrounding black squares show the borders of each box. The (forbidden) white space next to the borders has a width equal to the radius of the sphere; the white circles have a radius equal to that of the pins plus that of the sphere. (a) Experiment. (b) Simulations with $e_p=e_w=0.7$ [Fig. 4(b)]. (c) Simulations with $e_p=e_w=0.5$ [Fig. 4(a)]. (d) Simulations with $e_p=e_w=0.15$ [Fig. 8(a)]. (e) Simulations with $e_w=0.1$, $e_p=1$ [Fig. 8(b)].

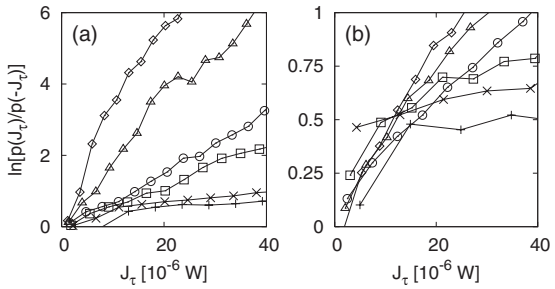

FIG. 8. Breakdown of linearity for $\ln[p(J_\tau)/p(-J_\tau)]$ vs J_τ, as obtained from simulations. Symbols for different τ are as in Fig. 3. (a) $e_p=e_w=0.15$; (b) $e_w=0.1$, $e_p=1$.

degree of disorder necessary for the FT is not given in this latter case.

As a test for the robustness of the results with respect to T, we reduced T to one-half; this yielded no significant change of any of the distributions $p(J_\tau)$.

IV. DISCUSSION

While Gaussian distributions $p(J_\tau)$ have been reported for some systems [9,13,23] we obtained non-Gaussian distributions $p(J_\tau)$, as in a large number of reported investigations (e.g., [18,21,22,24,25]). In our distributions of J_τ we obtain enhancements of $p(J_\tau)$ at J_τ near 0, which is due to the slowing down of the sphere after a collision. These enhancements cause no significant distortions of the linear plots.

We found that β_τ versus τ changes monotonically and saturates to a constant value for β_∞. This is in agreement with previous investigations. However, the approach to β_∞ differs in different systems: $d\beta/d\tau>0$ [9,14,17], $d\beta/d\tau\approx 0$ [22], or $d\beta/d\tau<0$ [23]. In the present system, $d\beta/d\tau<0$ for the experiments and for the simulations corresponding to Figs. 3–6, while for simulations with different parameters, e.g., for $e_w=1$ and $0.25<e_p<0.5$, the result is $d\beta/d\tau>0$. These discrepancies concerning the sign of $d\beta/d\tau$ remain to be clarified.

Figure 6 shows a clear monotonic dependence of β_∞ versus $\langle E_{kin}\rangle$. At least from that point of view, the consideration of β_∞ as a "temperature" makes some sense, although we are dealing here with a dissipative system out of equilibrium consisting of only one particle. An attempt to correlate β_∞ with $\langle E_{kin}\rangle$ had already been made by Feitosa and Menon [22] for a granular medium, for which $\beta_\infty/\langle E_{kin}\rangle\approx 5$ was obtained. For the results shown in Fig. 6, this quotient varies between 0.3 and 7.6.

The effective temperatures β_∞ obtained in simulations (Fig. 6) are much larger than the value obtained from experiments [Fig. 2(c)]. This is explainable by the omission of friction in the simulations. The omission of rotation and the reduction to two dimensions in the simulations may also influence the difference between experiments and simulations.

Another result of this work that is explainable by the omission of friction in the calculations is the fact that the best match to experiments (regarding spatial inhomogeneities and the validity of the FT) is obtained for restitution coefficients lower than expected, e.g., for $e_p=e_w=0.5$. In fact, values found in the literature are in the order of 0.8–0.9 [26] and yield homogeneous distributions [like Fig. 7(b)] in our calculations. This can be explained by assuming that the enhanced dissipation in our calculations (due to low e_p and e_w) compensates the missing friction.

V. CONCLUSIONS

In the derivation of the FT by Gallavotti and Cohen [5], a many-particle, time-reversible, chaotic Anosov system was assumed. It has also been shown that the FT is valid for dissipative systems [4,9,15,17,20]. In addition, it was shown that a many-particle system is not necessary if one assumes stochasticity [10–14]. In recent work [23], it was shown numerically that neither a many-particle system nor stochasticity is necessary, since the trajectory of a single, chaotically driven particle can be described by the FT. In the present work, we gave experimental evidence for this latter case and supported it with corresponding simulations. It is left to future work to determine the general conditions for a FT describing a single, driven particle, such as that in the experiments reported above.

ACKNOWLEDGMENT

We thank the Deutsche Forschungsgemeinschaft for Grant No. MA 629/6.

[1] G. Gallavotti, J. Math. Phys. **41**, 4061 (2000).
[2] D. J. Evans and D. J. Searles, Adv. Phys. **51**, 1529 (2002).
[3] C. Bustamante, J. Liphardt, and F. Ritort, Phys. Today **58**(7), 43 (2005).
[4] D. J. Evans, E. G. D. Cohen, and G. P. Morriss, Phys. Rev. Lett. **71**, 2401 (1993).
[5] G. Gallavotti and E. G. D. Cohen, Phys. Rev. Lett. **74**, 2694 (1995).
[6] F. Bonetto, G. Gallavotti, and P. L. Garrido, Physica D **105**, 226 (1997).
[7] S. Lepri, R. Livi, and A. Politi, Physica D **119**, 140 (1998).
[8] M. M. Sano, Phys. Rev. E **61**, 1144 (2000).
[9] A. Aumaître, S. Fauve, S. McNamara, and P. Poggi, Eur. Phys. J. B **19**, 449 (2001).
[10] J. Kurchan, J. Phys. A **31**, 3719 (1998).
[11] J. L. Lebowitz and H. Spohn, J. Stat. Phys. **95**, 333 (1999).
[12] P. Gaspard, J. Chem. Phys. **120**, 8898 (2004).
[13] R. van Zon and E. G. D. Cohen, Phys. Rev. E **67**, 046102 (2003).
[14] R. van Zon, S. Ciliberto, and E. G. D. Cohen, Phys. Rev. Lett. **92**, 130601 (2004).
[15] D. M. Carberry, J. C. Reid, G. M. Wang, E. M. Sevick, D. J.

Searles, and D. J. Evans, Phys. Rev. Lett. **92**, 140601 (2004).
[16] R. van Zon and E. G. D. Cohen, Phys. Rev. E **69**, 056121 (2004).
[17] S. Ciliberto and C. Laroche, J. Phys. IV **8**, 215 (1998).
[18] X.-D. Shang, P. Tong, and K.-Q. Xia, Phys. Rev. E **72**, 015301(R) (2005).
[19] S. Ciliberto, N. Garnier, S. Hernandez, C. Lacpatia, J.-F. Pinton, and G. Ruiz-Chavarria, Physica A **340**, 240 (2004).
[20] G. M. Wang, E. M. Sevick, E. Mittag, D. J. Searles, and D. J. Evans, Phys. Rev. Lett. **89**, 050601 (2002).
[21] N. Garnier and S. Ciliberto, Phys. Rev. E **71**, 060101(R) (2005).
[22] K. Feitosa and N. Menon, Phys. Rev. Lett. **92**, 164301 (2004).
[23] M. Schmick and M. Markus, Phys. Rev. E **70**, 065101(R) (2004).
[24] X.-D. Shang, X.-L. Qiu, P. Tong, and K.-Q. Xia, Phys. Rev. Lett. **90**, 074501 (2003).
[25] X.-D. Shang, X.-L. Qiu, P. Tong, and K.-Q. Xia, Phys. Rev. E **70**, 026308 (2004).
[26] S. F. Foerster, M. Y. Louge, H. Chang, and K. Allia, Phys. Fluids **6**, 1108 (1994).